Analytica Chimica Acta 1090 (2019) 91–99

Contents lists available at ScienceDirect

Analytica Chimica Acta

journal homepage: www.elsevier.com/locate/aca

Purification and characterization of thymol blue for spectrophotometric pH measurements in rivers, estuaries, and oceans

Ellie Hudson-Heck, Robert H. Byrne*

College of Marine Science, University of South Florida, 140 7th Avenue South, St. Petersburg, FL, 33701, USA

HIGHLIGHTS

- Thymol blue (TB) was purified using flash chromatography.
- TB is useful for pH measurements above the range of meta-cresol purple (mCP).
- Paired pH measurements directly link the equilibrium characteristics of TB and mCP.

GRAPHICAL ABSTRACT

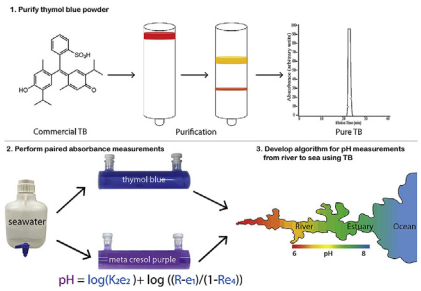

ARTICLE INFO

Article history:
Received 8 July 2019
Received in revised form
31 August 2019
Accepted 3 September 2019
Available online 11 September 2019

Keywords:
Thymol blue purification
Spectrophotometric pH
Estuarine conditions
Absorbance ratios

ABSTRACT

Thymol blue (TB) is one of a suite of indicator dyes appropriate for spectrophotometric determinations of the pH of aqueous solutions. For measurements of seawater pH, meta-cresol purple (mCP) is most often used, but TB is especially well suited for measurements in surface or shallow waters where the pH may exceed the optimal indicating range of mCP (e.g., due to photosynthesis). This work presents flash chromatography procedures for purifying commercially available TB and describes physical–chemical characteristics of the purified dye, thus enabling the acquisition of spectrophotometric pH measurements over a wide range of practical salinities (S_P) and temperatures (T). The essential TB characteristics for $0 \le S_P \le 40$ and $278.15 \le T \le 308.15$ K are described by:

$$pH_T = -_{TB}(\log(K_2^T e_2)) + \log((R - e_1)/(1 - Re_4))$$

$$_{TB}(\log(K_2^T e_2)) = 6.6942 - 0.001129S_p^{0.5}T - 0.5926T^{-0.5}S_p + 619.40/T + 0.1441S_P - 0.02591S_p^{1.5} + 0.0034S_p^2 - 0.0001754S_p^{2.5}$$

$$e_1 = -0.00132 + 0.00001600T$$

$$e_4 = -0.005042 + 0.0002094T + 0.01916S_P^{0.5}/T$$

where pH_T is pH determined on the total hydrogen ion concentration scale; R is the ratio of TB absorbances (A) at 435 and 596 nm ($_{596}A/_{435}A$); K_2^T is the equilibrium constant for the second TB dissociation step on the total scale; and e_1, e_2, and e_4 are TB molar absorptivity ratios. This characterization was developed in a manner that ensures consistency with the primary TRIS buffer standards used in previously published characterizations of mCP. With this characterization, TB joins mCP as a sulfonephthalein indicator that has been characterized over the ranges of salinity and temperature required to make high-quality pH measurements in rivers, estuaries, and the open ocean. The full characterization of purified TB reported here extends the upper range of pH_T that can be accessed with precise spectrophotometric measurements by approximately 0.50 pH units.

* Corresponding author.
E-mail addresses: rhbyrne@usf.edu, ehudsonheck@mail.usf.edu (R.H. Byrne).

https://doi.org/10.1016/j.aca.2019.09.009
0003-2670/

1. Introduction

The utility of spectrophotometric analyses of seawater pH was first demonstrated by Robert-Baldo et al. [1], who determined the pH-indicating characteristics of the sulfonephthalein indicator phenol red. In subsequent publications [1–3], the benefits of multiwavelength spectrophotometric pH measurements were demonstrated for both laboratory and shipboard applications. Since then, meta-cresol purple (mCP) has become the primary workhorse of open-ocean spectrophotometric pH measurements. The reproducibility that can be achieved using a dual-beam spectrophotometer is approximately ±0.0004 [3].

To measure pH spectrophotometrically, one must know the physical–chemical characteristics of a sulfonephthalein dye with a pH-indicating range that closely corresponds to the acidity of the samples of interest (e.g., natural seawater samples or natural samples modified by the addition of acid or base). As a general rule, a given indicator can be used for measurements over a range of approximately one to two pH units, with the indicator's dissociation characteristics roughly determining the midpoint of that range. For sample sets that encompass wider pH ranges, multiple indicators must be used.

The most accurate spectrophotometric pH measurements also require the use of purified indicator powder. Lot-specific light-absorbing impurities in off-the-shelf indicators may cause systematic pH errors as large as 0.015 [4,5]. Therefore, methods have been developed to purify commercial mCP by high-performance liquid chromatography (HPLC) [6] and commercial mCP and cresol red (CR) by a simple flash purification method [7].

The indicator most appropriate for full water-column measurements in the open ocean is mCP, with a pH-indicating range of approximately 7.0–8.4 at 25 °C and $S_P = 35$. In shallow coastal waters, however, pH values can be quite high, in excess of the optimal indicating range of mCP. For example, elevated pH attributable to the photosynthetic activity of macroalgae and seagrasses [8] has been widely observed, including values of up to 9.6 in Richardson Bay, California [9], 8.8 to 8.9 in shallow Danish waters [10], 8.9 to 9.6 in Tancada lagoon, Spain [11] and 8.9 in the seagrass meadows of Chwaka Bay, Zanzibar [12]. In order to better understand pH-dependent processes in high-pH waters, open-sea spectrophotometric methods must be modified [4] and the use of indicators other than mCP must be developed.

Thymol blue (TB), with an optimal pH-indicating range of approximately 7.5–8.9 (roughly 0.5 units higher than mCP), would be a strong addition to the toolbox of available dyes. This indicator (unpurified) was initially characterized for $30 \le S_P \le 40$ and $278.15 \le T \le 308.15$ K [13], with later extension to the wider salinity range of $0.06 \le S_P \le 40$ at 298.15 K [14]. Purified thymol blue has not been previously available.

Recently, the characterization of mCP has been linked to primary standards and also expanded to encompass conditions of $0 \le S_P \le 40$ and $278.15 \le T \le 308.15$ K, thus enabling measurements from river to sea within the indicating range of mCP [4,15]. These more complete descriptions also provide a means to characterize additional indicators and link them to primary standards through paired (concurrent) absorbance measurements with purified mCP.

This work describes a method to purify commercially available TB and introduces a model to describe the equilibrium and absorbance characteristics of purified TB over a wide range of environmental conditions ($0 \le S_P \le 40$ and $278.15 \le T \le 308.15$ K). Our procedures involve direct measurements of seawater pH using the mCP model of Müller and Rehder [15] to create a seamless transition between pH measurements obtained with mCP and the somewhat higher pH values that are more easily measured with TB. The overarching goal is to extend the upper limit of pH values that can be assessed with spectrophotometric procedures.

2. Theory

When thymol blue is added to a sample of seawater, the indicator partitions into the HI^- (yellow) and I^{2-} (blue) species shown in Fig. 1. From the ratio (R) of absorbances ($_\lambda A$) measured at wavelengths (λ) of 435 and 596 nm, the relative concentrations of the base and acid species can be determined and the solution pH_T (defined as $pH_T = [H^+]_F + [SO_4^{2-}]/K_{HSO4}^-$) can be calculated [1,2,6]:

$$pH_T = -\,{}_{TB}\left(\log\left(K_2^T e_2\right)\right) + \log\left((R - e_1)/(1 - Re_4)\right) \quad (1)$$

where pH_T is pH on the total hydrogen ion concentration scale; K_2^T is the equilibrium constant for the second TB dissociation step, expressed in terms of moles/kg of seawater; and $R = {}_{596}A/{}_{435}A$. The symbols e_1, e_2, e_3, and e_4 are ratios of molar absorptivity coefficients (i.e., expressions of light attenuation at specified wavelengths ($_\lambda\varepsilon$)) for the monoprotonated (HI^-) and fully deprotonated (I^{2-}) forms:

$$e_1 = {}_{596}\varepsilon_{HI^-} \Big/ {}_{435}\varepsilon_{HI^-}, \quad (2a)$$

$$e_2 = {}_{596}\varepsilon_{I^{2-}} \Big/ {}_{435}\varepsilon_{HI^-}, \quad (2b)$$

$$e_3 = {}_{435}\varepsilon_{I^{2-}} \Big/ {}_{435}\varepsilon_{HI^-}, \quad (2c)$$

$$e_4 = e_3/e_2 = {}_{435}\varepsilon_{I^{2-}} \Big/ {}_{596}\varepsilon_{I^{2-}} \quad (2d)$$

At sufficiently high pH where chemical forms of TB other than I^{2-} are negligible, the e_4 term is directly equivalent to the absorbance ratio A_{435}/A_{596}.

The values of ${}_{TB}(\log(K_2^T e_2))$ required in equation (1) can be determined over $0 \le S_P \le 40$ and $278.15 \le T \le 308.15$ K by measuring the pH_T of a sample solution with mCP and then also the absorbance ratio of TB in a second aliquot of the same solution:

$${}_{mCP}pH_T = {}_{TB}pH_T = -{}_{TB}\left(\log\left(K_2^T e_2\right)\right) + \log\left((R - e_1)/(1 - Re_4)\right) \quad (3)$$

The ${}_{mCP}pH_T$ of the solution can be calculated from absorbance measurements at 434 and 578 nm and the mCP model of Müller and Rehder [15].

3. Methods

3.1. Reagents and equipment

Meta-cresol purple (Tokyo Chemical lot XPPIF-JR) and thymol blue (Sigma Aldrich lot 04315 TC) sodium salts were purchased from Tokyo Chemical Industry and Sigma Aldrich. HPLC-grade acetonitrile was purchased from Fisher Scientific, and trifluoroacetic acid (TFA) was purchased from Sigma Aldrich. Sodium chloride (NaCl), potassium chloride (KCl), and calcium chloride ($CaCl_2$) were purchased from MP Biomedicals, Fisher Scientific, and Sigma Aldrich. The indicator powders were purified using a Teledyne ISCO CombiFlash Rf-200 UV-VIS automated flash chromatography system with a reversed-phase RediSep Gold C18 column (150 g). The purified column eluent was collected and then evaporated using a Buchi Rotavapor-R. Natural seawater was collected from the Gulf of Mexico.

Solution absorbance measurements were carried out on a Cary 400 Bio UV-VIS spectrophotometer paired with a Dell Optiplex

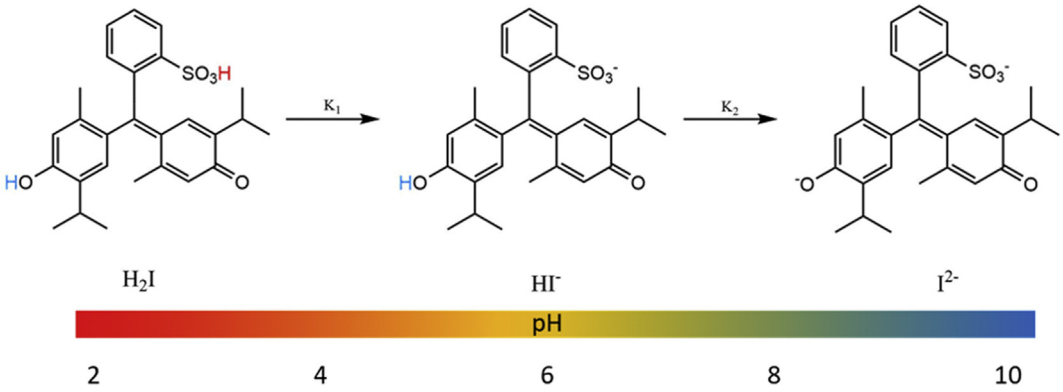

Fig. 1. Molecular structure of the diprotonated, monoprotonated, and deprotonated species of thymol blue. The color bar shows the color of each species in aqueous solution. (For interpretation of the references to color in this figure legend, the reader is referred to the Web version of this article.)

GX110 computer. Glass optical cells (10 cm pathlength) were filled using Teflon tubing directly connected to the end-cap of the cell. These cells were filled and then overflowed with sample seawater for 90 s to prevent gas exchange. The cells were equilibrated at desired temperatures in a thermostatted custom-made cell holder attached to a recirculating Thermo Scientific Neslab RTE 7 water bath. Indicator solution (mCP or TB) was added to the cells with a Gilmont micrometer syringe. The temperature of the seawater sample solutions was monitored using an Ertco-Eutechnics digital thermometer (±0.05 °C), which was calibrated against a Hewlett-Packard quartz thermometer probe. The practical salinity of each seawater batch was determined daily (±0.01) using a Guildline 8410A salinometer.

3.2. TB purification

Stock indicator solutions for the purification of TB were prepared by dissolving the commercial sodium salt in Milli-Q water (50 mM). The flash column was saturated with 5% acetonitrile prior to the start of each run. The solution of TB (20 mL) was then loaded onto the column with a plastic syringe. The column eluent, which was collected into a 500 mL round-bottom flask submerged in a waterbath, was subsequently evaporated at 40 °C. Finally, stock indicator solutions of purified TB were prepared by dissolving the purified solid (0.1 g) into Milli-Q water to achieve a final concentration of 10 mM. Sodium hydroxide (~200 μL, 1 M) was added to facilitate dissolution.

3.3. Absorbance measurement protocol

The following spectrophotometric protocol was used to determine e_4 and ${}_{TB}(\log(K_2^T e_2))$. Each optical cell was first equilibrated to its desired temperature. Next, an absorbance blank was recorded (sample solution with no added dye). Indicator dye was then injected (20 μL of TB for the e_4 determinations or 10 μL of mCP or TB for the ${}_{TB}(\log(K_2^T e_2))$ determinations), and the solution was fully mixed. Absorbance measurements were recorded at the absorbance maxima for the acid indicator form (i.e., ${}_{mCP}\lambda_{434}$ or ${}_{TB}\lambda_{435}$) and the base form (${}_{mCP}\lambda_{578}$ or ${}_{TB}\lambda_{596}$), as well as a non-absorbing wavelength (${}_{mCP}\lambda_{730}$ or ${}_{TB}\lambda_{750}$). To correct for potential baseline shifts due to possible changes in cell position, a baseline correction was applied [6,16]:

$$ {}_{TB}R = \frac{A_{596} - A_{750}}{A_{435} - A_{750}}, \quad {}_{mCP}R = \frac{A_{578} - A_{730}}{A_{434} - A_{730}} \tag{4} $$

The absorbance measurements were conducted over a range of temperatures, $278.15 \le T \le 308.15$ K, and the temperature of each seawater sample was recorded after each absorbance measurement. For temperatures below 15 °C, dry nitrogen gas was directed at the windows of the spectrophotometric cell in order to prevent condensation.

3.4. Determination of TB molar absorptivity ratios

Prior characterizations of e_1 for TB (equation (2a)) [13] demonstrated that $0.0031 \le e_1 \le 0.0036$ for temperatures between 5 and 35 °C. For absorbance ratios greater than 1 (i.e., $R \ge 1$), even ±50% errors in these e_1 estimates would create pH errors smaller than 0.001. Therefore, e_1 in this work was calculated using the characterization of Zhang and Byrne [13]: $e_1 = -0.00132 + 0.00001600T$.

The e_4 term for TB (equation (2d)) was characterized in artificial seawater over the salinity range $5 \le S_P \le 40$ and the temperature range $278.15 \le T \le 308.15$ K. At a pH of 12.5, the contribution from the HI^- species (Fig. 1) is negligible and values of e_4 could be obtained directly from absorbances measured at the wavelengths of the absorbance maxima of the acid and base forms (i.e., ${}_{TB}\lambda_{435}$ and ${}_{TB}\lambda_{596}$) [13].

For these measurements, stock artificial seawater medium was prepared according to a modification of the recipe provided by Delvalls and Dickson [17] for a salinity of 40. To avoid precipitation at high pH, the $MgCl_2$ and Na_2SO_4, of the original recipe were replaced with NaCl and $CaCl_2$. The stock medium was 0.568 M NaCl, 0.072 M $CaCl_2$, and 0.012 M KCl. To obtain a range of salinities below 40, the stock solution was gravimetrically diluted with Milli-Q water. To obtain the high-pH conditions under which e_4 could be measured directly, sodium hydroxide (6 M) was added to increase the pH of each solution to 12.5. The contribution of added NaOH was considered in the composition of each solution.

3.5. Determination of ${}_{TB}(\log(K_2^T e_2))$

To determine the ${}_{TB}(\log(K_2^T e_2))$ term required for equation (1), absorbance measurements were obtained for paired aliquots of identical seawater – one aliquot (spectrophotometric cell) with added mCP (purified and well-characterized) and one aliquot with added TB (purified but not yet well characterized). For each first aliquot, the pH_T of the solution was calculated by measuring the mCP absorbance ratio ($R = {}_{mCP}\lambda_{578}/{}_{mCP}\lambda_{434}$) and using equation 9 of Müller and Rehder [15] to calculate ${}_{mCP}(\log(K_2^T e_2))$ as a function of salinity and temperature. For each second aliquot, the TB absorbance ratio ($R = {}_{TB}\lambda_{596}/{}_{TB}\lambda_{435}$) was measured and equation (3) was used to calculate ${}_{TB}(\log(K_2^T e_2))$ as a function of salinity and

temperature.

For these measurements, natural seawater collected from the Gulf of Mexico (S_P ~35) was modified to obtain samples over a wide range of salinities. Higher salinities ($S_P > 35$) were achieved by evaporation. Lower salinities were achieved by dilution with deionized water. To increase the buffer intensity of the low-salinity samples ($S_P < 15$), $NaHCO_3$ was added to achieve a total concentration near 2 mM. After this addition, the salinity of the seawater was measured with the Guildline salinometer.

Duplicate dye injections were used to apply a perturbation correction to each value of R (i.e., to account for pH changes caused by adding the indicator dye) [3]. On average, the correction was 0.003 pH units. Additionally, to minimize this perturbation effect, the absorbance ratios of the mCP and TB stock solutions were adjusted with HCl (1 N) or NaOH (1 N) to match the approximate absorbance ratio of mCP and TB in each seawater solution.

The full ${}_{TB}(\log(K_2^T e_2))$ data set includes two subsets of data. For $2 \leq S_P \leq 40$, values of ${}_{TB}(\log(K_2^T e_2))$ were calculated from the paired mCP and TB absorbance measurements described above. For $0.06 \leq S_P \leq 4.98$, additional values of ${}_{TB}(\log(K_2^T e_2))$ were obtained by using the values of $\log((R-e_1)/(e_2-Re_3))$ and pH_T provided in Table 2 of Mosley et al. [14] (25 °C only) in conjunction with the e_2 value of Zhang and Byrne [13].

Multiple forms of polynomial fits (functional dependencies on salinity and temperature) were applied to the combined data set (Sigma Plot software, Systat). The significance of the addition or subtraction of a parameter was evaluated by using $P < 0.05$ and ensuring that the residual sum of squares (RSS) was at a minimum [4].

3.6. Determination of a simplified model for ${}_{mCP}(\log(K_2^T e_2))$

The fitting procedure described in section 3.5 was also used to fit the original mCP data of Müller and Rehder [15]. The goal of this refit was to examine the extent to which a simple predictive model of ${}_{mCP}(\log(K_2^T e_2))$, analogous to the simple predictive model of ${}_{TB}(\log(K_2^T e_2))$ described in section 3.5, could reproduce the capabilities of the full 19-parameter model of Müller and Rehder [15].

4. Results and discussion

4.1. Purification of thymol blue

Because the functional groups of TB are structurally similar to those of mCP and CR, it was expected that a procedure similar to that used by Patsavas et al. [7] to purify mCP and CR would be appropriate for TB. The published mCP and CR flash chromatographic methods use a mobile phase composition of acetonitrile, water, and 0.05% TFA as a modifier [7]. During our initial TB purification trials, however, it was observed that TFA may catalyze the formation of precipitates onto the stationary phase of the column. Therefore, TFA was excluded from the mobile phase for the TB procedure.

Table 1 shows the gradient mobile phase profile used to purify TB in which acetonitrile is incrementally increased to 22% and then held constant until the purified dye elutes from the column (~17 min). The final step, which increases the acetonitrile to 40% to eliminate any residue of TB from the column, is followed by a re-equilibration period that enables multiple injections. Comparison of the chromatograms of TB before and after purification (Fig. 2) demonstrates the capability of this method to eliminate impurities from commercially available powders.

The importance of purifying sulfonephthalein indicators for use in spectrophotometric pH_T measurements has been demonstrated in previous studies [5–7]. As shown in the chromatograms of Appendix A, different lots of commercially available TB powder contain different types and amounts of impurities. Off-the-shelf TB has distinctly lower levels of impurities than commercially available mCP and CR. Nevertheless, to ensure measurement accuracy, it is strongly recommended that (a) TB used for pH measurements be purified according to the procedure presented here, or (b) the procedures described by Douglas and Byrne [18] be utilized to quantitatively account for the absorbance contributions of impurities. These procedures are further discussed in section 4.7 below.

Table 1
Gradient mobile phase profile for purification of TB.

Time (min)	Acetonitrile (%)
0–1	5
1–6	5 to 22
6–19	22
19–21	40
21–25	5

Table 2
Parameters for use in calculating ${}_{TB}(\log(K_2^T e_2))$ as a function of S_P and T (equation (6)).

Parameter	Value
A	6.6942
B	−0.001129
C	−0.5926
D	619.40
E	0.1441
F	−0.02591
G	0.0034
H	−0.0001754

4.2. Salinity and temperature dependence of e_4

The modeled e_4 molar absorption characteristics of purified TB, obtained using observations for $5 \leq S_P \leq 40$ and $278.15 \leq T \leq 308.15$ K, are given by:

$$e_4 = -0.005042 + 0.0002094T + 0.01916\, S_P^{0.5}/T \quad (5)$$

Fig. 3 shows the resulting residuals as a function of salinity and temperature.

Table C1 (in Appendix C) compares this work's direct measurements of e_4 with values calculated from the e_2 and e_3 results of Zhang and Byrne [13] for $S_P = 35$. Fig. C1 compares the results of equation (5) with the results of Zhang and Byrne [13] as a function of S_P and T. On average, the e_4 values predicted in this work are only about 1% lower than the earlier values ($30 \leq S_P \leq 40$), even though commercial (i.e., unpurified) TB was used for that work and purified TB was used for this work. For $0.2 \leq R \leq 5$, the small difference in e_4, potentially attributable to impurities in the indicator of Zhang and Byrne [13], would result in a pH_T difference no greater than 0.0023 for $5 \leq S_P \leq 40$ and $T = 298.15$ K. This excellent e_4 agreement is consistent with earlier observations [6] that the low levels of impurities found in the commercial TB used by Zhang and Byrne [13] had minimal effects on absorbance measurements at 435 and 596 nm.

4.3. Parameterization of ${}_{TB}(\log(K_2^T e_2))$

As noted in section 3.5, the data set used to parameterize ${}_{TB}(\log(K_2^T e_2))$ is a compilation of experimental values obtained in this study ($2 \leq S_P \leq 40$) plus additional values calculated from the low-salinity ($0.06 \leq S_P \leq 4.98$) data of Mosley et al. [14]. The full

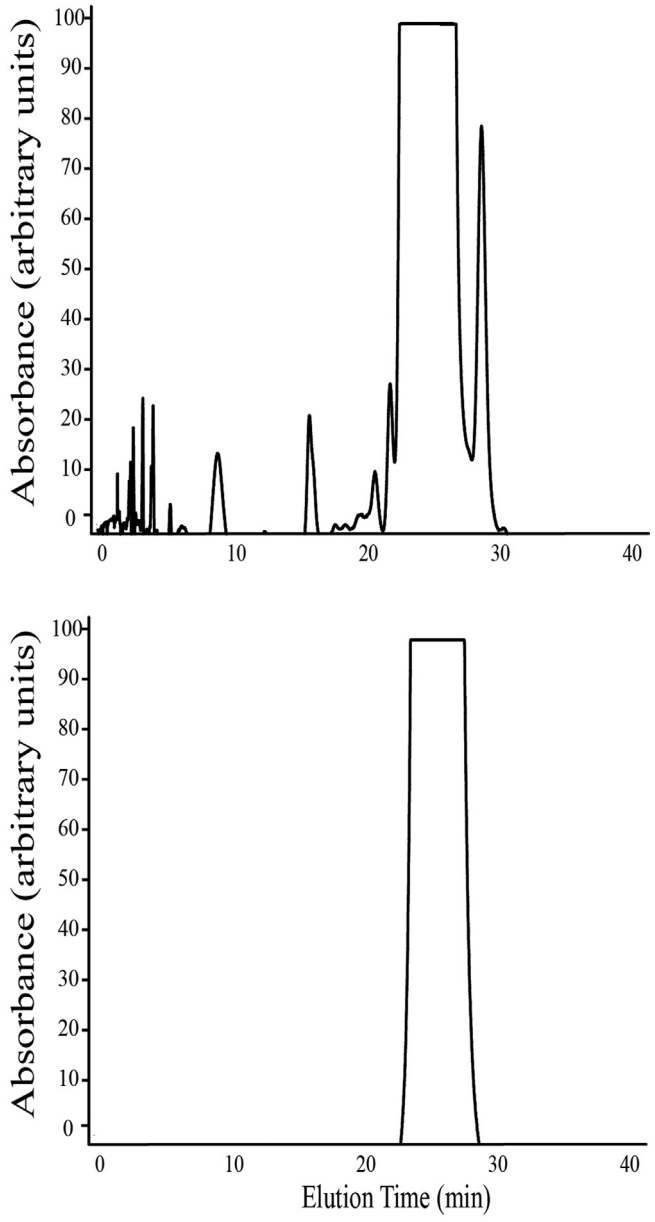

Fig. 2. HPLC chromatograms of (top) off-the-shelf TB (Sigma Aldrich lot 04315 TC) and (bottom) purified TB, obtained after flash chromatographic purification using the gradient profile given in Table 1.

compilation is provided in Table B2 of Appendix B.

The salinity and temperature dependence of $_{TB}(\log(K_2^T e_2))$ is well described by:

$$_{TB}\left(\log\left(K_2^T e_2\right)\right) = A + BS_p^{0.5}T + CT^{-0.5}S_P + D/T + ES_P + FS_p^{1.5} + GS_p^2 + HS_p^{2.5} \quad (6)$$

with the parameters given in Table 2. For salinity 35.00 and temperature 298.15 K, equation (6) yields $_{TB}(\log(K_2^T e_2)) = 8.1514$. As a quality-control check, investigators using equation (6) should confirm that their computations yield this value.

Although Mosley et al. [14] used unpurified TB, we opted to use their data to augment the range of salinities covered by our own measurements because (a) only low levels of impurities are typically present in off-the-shelf TB and (b) their observations at $0.06 \le S_P \le 4.98$ were obtained under conditions that created a very large HI^-/I^{2-} concentration ratio (between approximately 5 and 10), such that pH errors attributable to impurities would have been substantially minimized [4,5]. As shown in Fig. 4, the similar magnitudes of residuals for the two subsets of data within the salinity range of overlap ($2 \le S_P \le 5$) indicate that the influence of impurities on the Mosley et al. [14] TB measurements we used was small.

Fig. C2 (Appendix C) shows the difference between values of $_{TB}(\log(K_2^T e_2))$ predicted from equation (6) and values calculated from Zhang and Byrne [13]. At 298.15 K, the difference between the two models is within ±0.0006 for $30 \le S_P \le 40$. Therefore, the results of previous studies that used the TB parameterization of Zhang and Byrne [13] to obtain pH_T at 298.15 K will not be significantly changed by using our model instead. The largest discrepancies are found at high salinity and temperature extremes. The maximum difference in $_{TB}(\log(K_2^T e_2))$ between the two models is −0.0055, which is seen at salinity 40 and temperature 278.15 K.

The equilibrium characteristics of indicator dyes should be linked to primary pH standards to ensure consistency across all spectrophotometric pH_T measurements. Our TB model is linked to primary standards through the $_{mCP}pH_T$ values calculated using the mCP model of Müller and Rehder [15] (see equation (3)). In their characterization of mCP, they utilized Harned cell measurements to determine the pH_T of their TRIS buffer solutions [19]. The data provided in Appendix B (Table B2) include values of S_P, T, $_{mCP}pH_T$, and $_{TB}R$. If the mCP model of Müller and Rehder [15] is revised in the future, the data of Table B2 (with recalculated values of $_{mCP}pH_T$) will be sufficient to construct a new TB model consistent with that revision.

4.4. Simplified model for $_{mCP}(\log(K_2^T e_2))$

The mCP data set compiled by Müller and Rehder [15] provides a robust description of $_{mCP}(\log(K_2^T e_2))$ over a wide range of salinities and temperatures, with an accompanying 19-parameter model for predicting $_{mCP}(\log(K_2^T e_2))$ as a function of S_P and T. Given that the 8-parameter $_{TB}(\log(K_2^T e_2))$ model of this study (equation (6)) performs well with a random distribution of small residuals (Fig. 4), we examined the extent to which a similar $_{mCP}(\log(K_2^T e_2))$ model could describe the Müller and Rehder [15] mCP data.

The approach was to fit a modified form of the TB model (equation (6)) to the entire mCP data set of Müller and Rehder [15] ($0 \le S_P \le 40$, $278.15 \le T \le 308.15$ K). The resulting model requires 7 parameters:

$$\mathrm{mCP}\left(\log\left(K_2^T e_2\right)\right) = A + B/T + ((CS_p^{0.5} + DS_P)/T^{1.5} + ES_p^{1.5}) / (1 + FS_P/T)) + GS_P \quad (7)$$

with the parameter values given in Table 3. For salinity 35.00 and temperature 298.15 K, equation (7) yields $_{mCP}(\log(K_2^T e_2)) = 7.6466$.

This model yields an RSS of 0.0006, which is twice the 0.0003 RSS obtained with the original parameterization of Müller and Rehder [15]. Within the ranges of $4 \le S_p \le 40$ and $278.15 \le T \le 303.15$, equation (7) agrees with the Müller and Rehder [15] model to within ±0.002 (Fig. 5). The largest differences are seen at $S < 4$. The maximum offset (−0.0066) occurs at $S_P = 1$ and $T = 278.15$ K. At low salinities, achieving an accurate pH measurement is more difficult due to the large changes seen in $\log(K_2^T e_2)$ in response to only small changes in S_P [4,20].

Although equation (7) and Table 3 provide an acceptable means of determining pH with mCP in estuarine waters at $T \le 303.15$, the 19-parameter model of Müller and Rehder [15] does, of course, provide a superior description of available calibration data. As such,

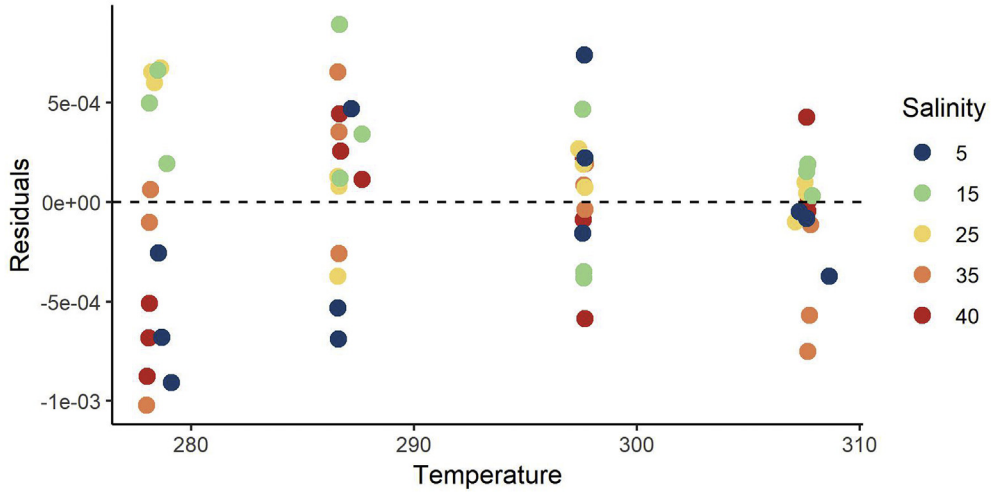

Fig. 3. Residuals for the e_4 model fit. The experimental data are listed in Appendix B (Table B1).

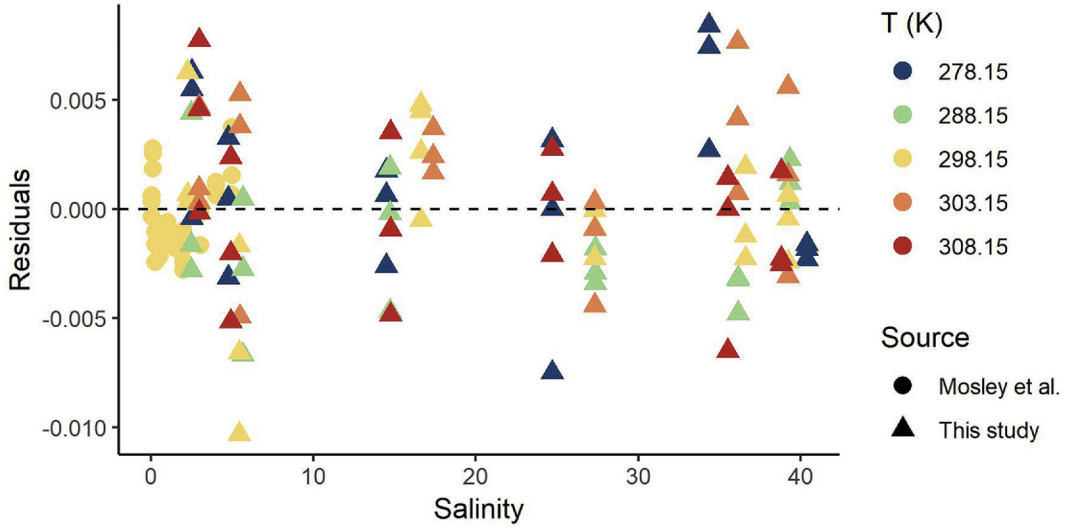

Fig. 4. Residuals for the $_{TB}(\log(K_2^T e_2))$ model fit (equation (6)). Overall, 95% of the residuals are within ±0.007. The full data set is given in Table B2.

while the Müller and Rehder [15] model should be the preferred model for calculations, the results shown in Fig. 5 provide important perspectives on the level of accuracy that can be achieved with relatively simple descriptions of the physical-chemical behavior of sulfonephthalein indicators.

4.5. Indicating ranges of TB and mCP

The coupled mCP and TB absorbance measurements used in this work ensures that our $_{TB}pH_T$ model is closely linked to the rigorous and well-documented $_{mCP}pH_T$ model of Müller and Rehder [15]. This coupling is highly desirable because it ensures not only a link to primary standards but also a smooth transition between pH measurements obtained with the two indicators. There is not a discrete pH value at which an investigator must switch from one indicator to the other.

As noted in section 1, the indicating range of a given sulfonephthalein dye is determined primarily by the dissociation constant that describes the H^+ exchange reaction being quantified by absorbance measurements. The midrange of the pH indicating range will be approximately equal to that pK value, and the width of the range will be approximately one to two pH units. Higher-quality spectrophotometers can capably handle a greater range of $_{\lambda}A$, thereby providing a wider indicating range [1,3,21,22].

Another way to think about optimal indicating ranges is in terms of the absorbance ratio R, which is at the core of the spectrophotometric pH method (equation (1)). For any indicator, with increasing pH, R approaches a value equal to $(e_4)^{-1}$, the denominator of equation (1) term $(R - e_1)/(1 - Re_4)$ approaches zero, and

Table 3
Parameters for use in calculating $_{mCP}(\log(K_2^T e_2))$ from equation (7), based on the data of Müller and Rehder [15].

Parameter	Value
A	5.60179
B	803.9272
C	−0.32595
D	85.2429
E	−0.06120
F	95.8923
G	0.014068

systematic inaccuracies in pH_T calculations can develop. Because Re_4 must, by definition, be ≤ 1, each sulfonephthalein indicator has an upper-bound R value that cannot be exceeded: i.e., R must be $\leq (e_4)^{-1}$. At 25 °C and $S_P = 35$, ${}_{mCP}R$ must be ≤ 17.61 and ${}_{TB}R$ must be ≤ 17.30. For identical values of R_{mCP} and R_{TB} up to $R = 15$, the corresponding values of pH calculated with the two indicators differ by approximately 0.50 pH units: i.e., ${}_{TB}pH = {}_{mCP}pH + 0.50$. Thus, for a given R value, higher pH values can be more reliably measured with TB than with mCP.

The choice of an R value where an investigator should consider transitioning from mCP to TB (or vice versa) depends on the quality of the spectrophotometer being used. For a relatively inexpensive spectrophotometer, stray light problems at high absorbances (created by high R values) can cause deviations from Beers Law (i.e., nonlinearity in absorbance as a function of concentration). This nonlinearity will create inaccuracy in R measurements without necessarily affecting measurement precision. Whatever upper-bound R value is chosen for mCP measurements at a given salinity and temperature, it should be noted that TB will allow for measurements at pH values that are approximately 0.50 pH units higher by those allowed for by mCP.

4.6. pH accuracy

Because no standards are currently available for directly assessing pH accuracy, the quality of pH measurements is generally assessed (explicitly or implicitly) in terms of their consistency with measurements of other carbon dioxide system variables [23–26]: total alkalinity (TA), total dissolved inorganic carbon (DIC), and CO_2 fugacity (f_{CO2}). Measurements of any two CO_2 system variables can be used to calculate all other CO_2 system variables [27], including pH.

For pelagic conditions, comparisons of measured and calculated CO_2 system variables exhibit very good but imperfect agreement. For example, measured values of TA in the pelagic ocean generally exceed values predicted from paired DIC and spectrophotometric pH_T measurements by approximately 4–6 μmol/kg. Uncertainties in quantities incorporated into the calculations could be contributing to this discrepancy: e.g., uncertainties in CO_2 system dissociation constants (K_1 and K_2), the dissociation constant of boric acid, and the seawater ratio of boron to salinity. Another possible source of discrepancy might be the contributions of organic bases to seawater alkalinity [26], which are generally assumed to be zero (or at least are not explicitly accounted for).

Because the present work endeavored to closely link the properties of TB to those of mCP, it is expected that seawater pH measurements with TB will produce differences between CO_2 system measured and calculated quantities in close agreement with assessments obtained with mCP. To date, the number of internal consistency measurements obtained with TA, DIC, and ${}_{mCP}pH_T$ is in the tens of thousands. To our knowledge, no such studies have yet been published for TB. Therefore, the inclusion of ${}_{TB}pH_T$ for paired measurements and consistency checks of TA, DIC, and pH_T in the surface ocean should be encouraged over broad ranges of salinity and temperature. Nearly all previous comparisons have been made in pelagic waters, so expanding internal consistency evaluations to riverine and estuarine systems would be of special value.

4.7. Correcting for the use of impure TB

Because the level of impurities is generally low in commercial lots of thymol blue, the use of purified TB is not necessarily required to ensure accurate pH measurements in natural waters. As a simple means of not only assessing the purity of TB but also, when necessary, mitigating the influence of TB impurities on pH calculations, the procedures used by Douglas and Byrne [18] for mCP can be used. The basic approach is to correct R values obtained using unpurified indicator to values consistent with the use of a purified batch of that same indicator. The key requirement (for either TB or mCP) is to compare measurements of e_4 obtained with off-the-shelf (unpurified) indicator against e_4 characterizations obtained with the purified indicator. The difference between these two measurements can then be used to correct for the contributions of impurities to R values obtained using an unpurified indicator [18].

For TB, e_4 results for the pure indicator are given in equation (5). Accordingly, if unpurified TB is to be used (or has been used) for pH_T measurements, the protocol provided in Table 1 of Douglas and Byrne [18] can be used with two essential changes: (1) in their Step 2, the pH of ~12 for mCP assessment should be changed to a pH of 12.5 for TB assessment, and (2) In their step 8, the value of e_3/e_2 (i.e., $e_3/e_2 = e_4$; equation (2d)) should be calculated for TB from equation (5) of this work. Degradation of purified TB that was stored without protection from laboratory light was not observed in this study. However long-term assessment of photochemical or microbial

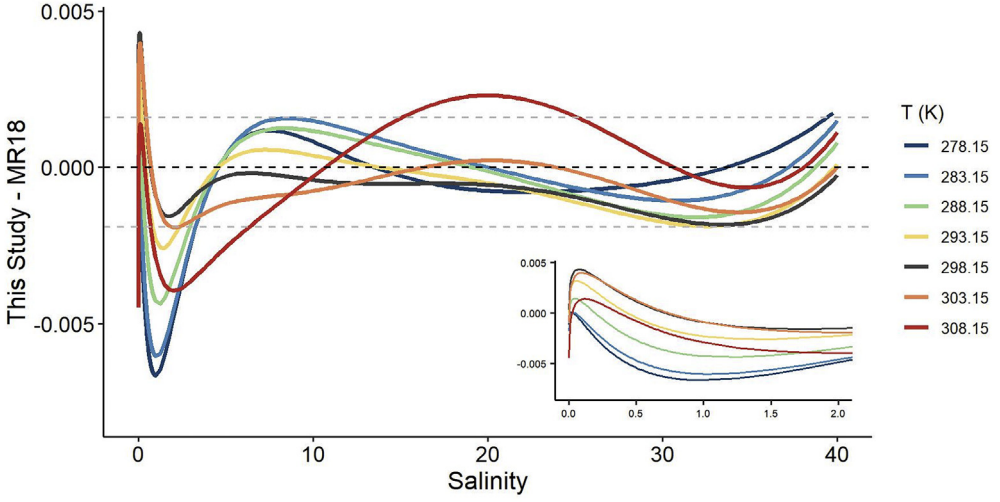

Fig. 5. Differences between the values of ${}_{mCP}(\log(K_2^T e_2))$ predicted from the model fit of this study (equation (7)) and the model fit of Müller and Rehder [15] (their equation 9). The inset panel gives an expanded view of the differences for $S < 4$.

degradation of sulphonephthalein dyes is ongoing.

5. Conclusions and implications

This work's characterization of the pH-indicating properties of thymol blue extends the range of pH measurements that can be obtained with purified indicators by approximately 0.5 pH units across a river-to-sea range of temperatures and salinities. TB is well suited for measuring pH in the surface ocean, especially for examinations of diel pH variations in shallow waters where intense photosynthetic activity can produce high pH values and CO_2 partial pressures that are much below atmospheric pCO_2.

As indicated by equation (6), values of ${}_{TB}(\log(K_2^T e_2))$ change by approximately 0.013 for a 1 °C change in temperature. (The same is true for the analogous log term of most sulfonephthalein indicators.) As such, measuring temperature to within ±0.1 °C would be sufficient to achieve a seawater pH_T measurement precision of 0.0013 pH units. As noted previously, however [2,3], due to the similar temperature dependencies of sulfonephthalein dissociation constants and seawater pH (both ~0.014 per °C), temperature uncertainties on the order of ±0.1 °C do not contribute significantly to the typical ± 0.001 imprecision of spectrophotometric pH measurements.

The value of $\log(K_2^T e_2)$ is most sensitive to salinity at $S_P < 5$ (Fig. 5). At 25 °C, for an increase in salinity between 0 and 5, ${}_{TB}(\log(K_2^T e_2))$ decreases by 0.418; between 5 and 40, the change is only 0.209. The strong salinity dependence of $\log(K_2^T e_2)$ for $S_P < 5$ mirrors the salinity dependence of the carbonic acid dissociation constants (K_1 and K_2) over the same salinity range. As an example, $\log K_2$ values for the dissociation of HCO_3^- at 25 °C decreases by 0.687 between $S_P = 0$ and $S_P = 5$ [28], thus mirroring the behavior of the thymol blue $\log(K_2^T e_2)$ term. This correlation of dependencies on S_P diminishes the potential for salinity-induced errors in carbon dioxide system calculations.

As has been demonstrated for mCP, algorithms describing the molecular properties of indicators are subject to ongoing refinement [4,15]. Through the use of (a) purified indicators and (b) archived values of R, S_P, and T for every sample, any original values of pH_T (and any subsequently derived carbon dioxide system quantities) can be redetermined using the updated indicator algorithms [3]. This advantage, which cannot be achieved with glass electrodes, is especially important in an era of long-term environmental monitoring. This benefit is also a contributing factor that underlies ongoing global efforts to purify and characterize additional indicator dyes for measuring solution pH in a variety of aquatic environments.

Declaration of competing interest

The authors declare that they have no known competing financial interests or personal relationships that could have appeared to influence the work reported in this paper.

Acknowledgements

Support for this work was provided by the National Science Foundation (award OCE-1657894) and the C.W. Bill Young Fellowship Program Fund of the University of South Florida, College of Marine Science. We would like to thank Dr. Jens D. Müller and Dr. Gregor Rehder for providing their mCP data set for use in this work. We would also like to thank Dr. Tonya Clayton for her editing and constructive criticism of this manuscript. The authors gratefully acknowledge the comments of two anonymous reviewers.

Appendix A. Supplementary data

Supplementary data to this article can be found online at https://doi.org/10.1016/j.aca.2019.09.009.

References

[1] R.H. Byrne, G. Robert-Baldo, S.W. Thompson, C.T.A. Chen, Seawater pH measurements: an at-sea comparison of spectrophotometric and potentiometric methods, Deep Sea Research Part A, Oceanogr. Res. Pap. 35 (1988) 1405–1410, https://doi.org/10.1016/0198-0149(88)90091-X.
[2] R.H. Byrne, J.A. Breland, High precision multiwavelength pH determinations in seawater using cresol red, Deep Sea Research Part A, Oceanogr. Res. Pap. 36 (1989) 803–810, https://doi.org/10.1016/0198-0149(89)90152-0.
[3] T.D. Clayton, R.H. Byrne, Spectrophotometric seawater pH measurements: total hydrogen ion concentration scale calibration of m-cresol purple and at-sea results, Deep Sea Res. Oceanogr. Res. Pap. 40 (1993) 2115–2129, https://doi.org/10.1016/0967-0637(93)90048-8.
[4] N.K. Douglas, R.H. Byrne, Spectrophotometric pH measurements from river to sea: calibration of mCP for $0 \leq S \leq 40$ and $278.15 \leq T \leq 308.15$K, Mar. Chem. 197 (2017) 64–69, https://doi.org/10.1016/j.marchem.2017.10.001.
[5] W. Yao, X. Liu, R.H. Byrne, Impurities in indicators used for spectrophotometric seawater pH measurements: assessment and remedies, Mar. Chem. 107 (2007) 167–172, https://doi.org/10.1016/j.marchem.2007.06.012.
[6] X. Liu, M.C. Patsavas, R.H. Byrne, Purification and characterization of meta-cresol purple for spectrophotometric seawater pH measurements, Environ. Sci. Technol. 45 (2011) 4862–4868, https://doi.org/10.1021/es200665d.
[7] M.C. Patsavas, R.H. Byrne, X. Liu, Purification of meta-cresol purple and cresol red by flash chromatography: procedures for ensuring accurate spectrophotometric seawater pH measurements, Mar. Chem. 150 (2013) 19–24, https://doi.org/10.1016/j.marchem.2013.01.004.
[8] P. Buapet, L.M. Rasmusson, M. Gullström, M. Björk, Photorespiration and carbon limitation determine productivity in temperate seagrasses, PLoS One 8 (2013), https://doi.org/10.1371/journal.pone.0083804 e83804.
[9] W.A. Setchell, Ruppia and its environmental factors, Proc. Natl. Acad. Sci. U. S. A 10 (1924) 286, https://doi.org/10.1073/pnas.10.6.286.
[10] A.L. Middelboe, P.J. Hansen, High pH in shallow-water macroalgal habitats, Mar. Ecol. Prog. Ser. 338 (2007) 107–117, https://doi.org/10.3354/meps338107.
[11] M. Menéndez, M. Martınez, F.A. Comın, A comparative study of the effect of pH and inorganic carbon resources on the photosynthesis of three floating macroalgae species of a Mediterranean coastal lagoon, J. Exp. Mar. Biol. Ecol. 256 (2001) 123–136, https://doi.org/10.1016/S0022-0981(00)00313-0.
[12] I.S. Semesi, J. Kangwe, M. Björk, Alterations in seawater pH and CO_2 affect calcification and photosynthesis in the tropical coralline alga, Hydrolithon sp. (Rhodophyta), Estuarine, Coast Shelf Sci. 84 (2009) 337–341, https://doi.org/10.1016/j.ecss.2009.03.038.
[13] H. Zhang, R.H. Byrne, Spectrophotometric pH measurements of surface seawater at in-situ conditions: absorbance and protonation behavior of thymol blue, Mar. Chem. 52 (1996) 17–25, https://doi.org/10.1016/0304-4203(95)00076-3.
[14] L.M. Mosley, S.L.G. Husheer, K.A. Hunter, Spectrophotometric pH measurement in estuaries using thymol blue and m-cresol purple, Mar. Chem. 91 (2004) 175–186, https://doi.org/10.1016/j.marchem.2004.06.008.
[15] J.D. Müller, G. Rehder, Metrology of pH measurements in brackish waters—Part 2: experimental characterization of purified meta-cresol purple for spectrophotometric pH_T measurements, Front. Mar. Sci. 5 (2018), https://doi.org/10.3389/fmars.2018.00177.
[16] M.C. Patsavas, R.H. Byrne, X. Liu, Physical–chemical characterization of purified cresol red for spectrophotometric pH measurements in seawater, Mar. Chem. 155 (2013) 158–164, https://doi.org/10.1016/j.marchem.2013.06.007.
[17] T.A. DelValls, A.G. Dickson, The pH of buffers based on 2-amino-2-hydroxymethyl-1,3-propanediol ('tris') in synthetic sea water, Deep Sea Research Part I, Oceanogr. Res. Pap. 45 (1998) 1541–1554, https://doi.org/10.1016/S0967-0637(98)00019-3.
[18] N.K. Douglas, R.H. Byrne, Achieving accurate spectrophotometric pH measurements using unpurified meta-cresol purple, Mar. Chem. 190 (2017) 66–72.
[19] J.D. Müller, F. Bastkowski, B. Sander, S. Seitz, D.R. Turner, A.G. Dickson, G. Rehder, Metrology for pH measurements in brackish waters—Part 1: extending electrochemical pH_T measurements of TRIS buffers to salinities 5–20, Front. Mar. Sci. 5 (2018), https://doi.org/10.3389/fmars.2018.00176.
[20] C.-Z. Lai, M.D. DeGrandpre, B.D. Wasser, T.A. Brandon, D.S. Clucas, E.J. Jaqueth, Z.D. Benson, C.M. Beatty, R.S. Spaulding, Spectrophotometric measurement of freshwater pH with purified meta-cresol purple and phenol red, Limnol Oceanogr. Methods. 14 (n.d.) 864–873. doi:10.1002/lom3.10137.
[21] R.H. Byrne, Standardization of standard buffers by visible spectrometry, Anal. Chem. 59 (1987) 1479–1481, https://doi.org/10.1021/ac00137a025.
[22] W. Yao, R.H. Byrne, Spectrophotometric determination of freshwater pH using bromocresol purple and phenol red, Environ. Sci. Technol. 35 (2001) 1197–1201, https://doi.org/10.1021/es001573e.
[23] F.J. Millero, R.H. Byrne, R. Wanninkhof, R. Feely, T. Clayton, P. Murphy, M.F. Lamb, The internal consistency of CO_2 measurements in the equatorial

Pacific, Mar. Chem. 44 (1993) 269–280, https://doi.org/10.1016/0304-4203(93)90208-6.
[24] T.D. Clayton, R.H. Byrne, J.A. Breland, R.A. Feely, F.J. Millero, D.M. Campbell, P.P. Murphy, M.F. Lamb, The role of pH measurements in modern oceanic CO_2-system characterizations: precision and thermodynamic consistency, Deep Sea Res. Part II Top. Stud. Oceanogr. 42 (1995) 411–429, https://doi.org/10.1016/0967-0645(95)00028-O.
[25] M.C. Patsavas, R.H. Byrne, R. Wanninkhof, R.A. Feely, W.-J. Cai, Internal consistency of marine carbonate system measurements and assessments of aragonite saturation state: insights from two U.S. coastal cruises, Mar. Chem. 176 (2015) 9–20, https://doi.org/10.1016/j.marchem.2015.06.022.
[26] M.B. Fong, A.G. Dickson, Insights from GO-SHIP hydrography data into the thermodynamic consistency of CO_2 system measurements in seawater, Mar. Chem. 211 (2019) 52–63, https://doi.org/10.1016/j.marchem.2019.03.006.
[27] A.G. Dickson, C. Goyet, Handbook of Methods for the Analysis of the Various Parameters of the Carbon Dioxide System in Sea Water, Oak Ridge National Lab., TN (United States), 1994, https://doi.org/10.2172/10107773. Version 2.
[28] F.J. Millero, T.B. Graham, F. Huang, H. Bustos-Serrano, D. Pierrot, Dissociation constants of carbonic acid in seawater as a function of salinity and temperature, Mar. Chem. 100 (2006) 80–94, https://doi.org/10.1016/j.marchem.2005.12.001.